Inorganica Chimica Acta xxx (2016) xxx–xxx

Contents lists available at ScienceDirect

Inorganica Chimica Acta

journal homepage: www.elsevier.com/locate/ica

Research paper

Synthesis, electrochemical, structural and theoretical study of new derivatives of O—B—N and O—B—O heterocycles

Tomáš Mikysek [a], Hana Kvapilová [b], Hana Doušová [c], František Josefík [c], Petr Šimůnek [c], Zdeňka Růžičková [d], Jiří Ludvík [b,*]

[a] University of Pardubice, Faculty of Chemical Technology, Department of Analytical Chemistry, Studentská 573, Pardubice CZ 532 10, Czech Republic
[b] J. Heyrovský Institute of Physical Chemistry, ASCR, v.v.i., Dolejškova 3, 182 23 Prague 8, Czech Republic
[c] University of Pardubice, Faculty of Chemical Technology, Institute of Organic Chemistry and Technology, Studentská 573, Pardubice CZ 532 10, Czech Republic
[d] University of Pardubice, Faculty of Chemical Technology, Department of General and Inorganic Chemistry, Studentská 573, Pardubice CZ 532 10, Czech Republic

ARTICLE INFO

Article history:
Received 13 April 2016
Received in revised form 4 August 2016
Accepted 5 August 2016
Available online xxxx

Keywords:
Boron heterocycles
Synthesis
X-ray structure analysis
Electrochemistry
HOMO-LUMO
DFT calculations

ABSTRACT

Three new oxazaborine and two boron diketonate derivatives containing different structural motifs were synthesized and studied using NMR, electrochemistry (CV, RDV, and dc-polarography), UV–Vis spectra and X-ray structure analysis. The experimental data were correlated with quantum chemical calculations. The main attention was focused on determination of the first oxidation and the first reduction potentials, their relationship to the calculated HOMO and LUMO energies and to their UV–Vis spectra. The electrochemical data reflect the structure–redox properties relationship depending on location of oxidation and reduction center.

1. Introduction

Since the second half of the last century, when the chemistry of boron-containing heterocycles was born [1–3], it has been experiencing a significant expansion. Boron heterocycles were promoted from relative curiosities into compounds having a broad spectrum of useful properties. The presence of boron in the molecules of organic compounds substantially changes their electronic properties in comparison with the carbocyclic analogues [4]. Many boron-containing heterocycles have great potential for applications in molecular electronics as non-linear optical (NLO) chromophores and OLED materials [5,6]. A great chapter of boron heterocycles are BODIPY, highly fluorescent and stable compounds suitable as dyes, sensors and materials for OLEDs [7,8]. Some N—B—O heterocycles have been considered for using in BNCT (boron-neutron capture therapy) [9]. Some compounds of this type possess antibacterial activity [10].

During past several years we have developed a simple methodology for synthesis of various kinds of O—B—N and N—B—N heterocycles with BPh_2 moiety from corresponding polarized ethylenes [11–14]. In addition to the synthesis we have been studying the properties of some of the heterocycles prepared as well. A number of bicyclic triazaborines exhibit fluorescence in powder and 2-MeTHF frozen state [14]. Recently we have performed electrochemical and DFT study of a homologous series of bicyclic triazaborines [15a] and their precursors, oxazaborines [15b]. The obtained results describe and compare redox properties of both series, their HOMO and LUMO energies, localization of redox centers within the molecules and relationship between the structure and properties, which could be used for both the understanding the electronic situation inside the heterocycles and for tuning-up their properties so as to be tailored for particular application.

The present work represents a convenient extension of the previous contributions. It deals with synthesis, electrochemical and quantum chemical study of three oxazaborines (boron ketoiminates) being analogous to those in our previous study but without the *p*-substituted phenyl azo-pendant (**5a**–**c**) and two similar boron diketonates (**4a**,**b**). The oxazaborine **6** [15b] was taken for direct comparison with its homologue **5c** as a "bridging" compound interconnecting the previous and the present series of compounds. (Scheme 1).

* Corresponding author.
E-mail address: jiri.ludvik@jh-inst.cas.cz (J. Ludvík).

http://dx.doi.org/10.1016/j.ica.2016.08.009
0020-1693/

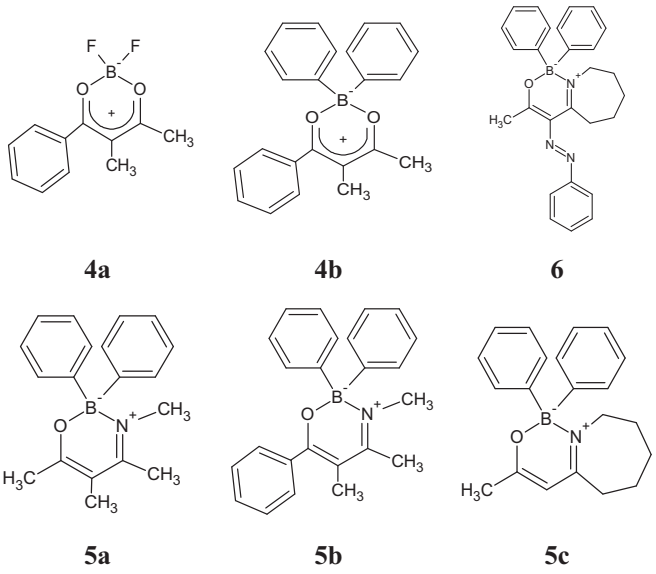

Scheme 1. Oxazaborines and boron diketonates studied in this work.

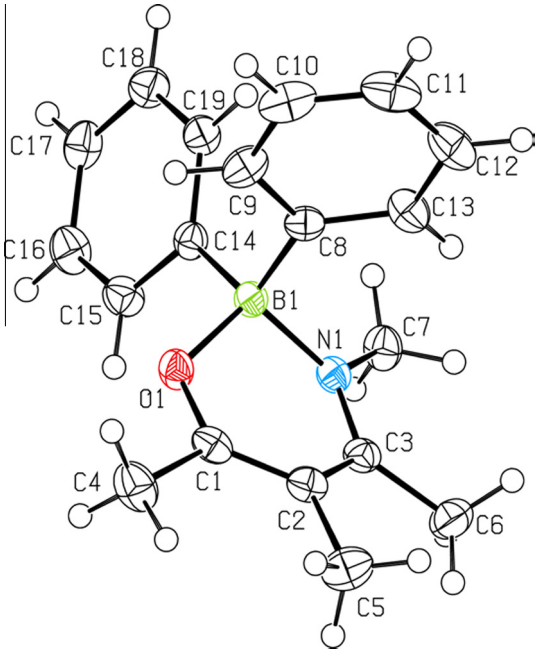

Fig. 1. The molecular structure (ORTEP 50% probability level) of **5a**.

2. Results and discussion

2.1. Synthesis

Boron diketonates **4a**,**b** and ketoiminates **5a**–**c** involved in the study were prepared according to the Scheme 2. The BR_2 fragment was introduced by means of the reaction of appropriate trivalent boron compound (BF_3, BPh_3 or Ph_2BOH) with β-diketone or β-enaminone. The synthesis of enaminone **3a** was done using classic condensation between 3-methylacetylacetone (**1a**) and methylamine. An attempt to prepare in the same way also its benzoylacetone analogue **3b** failed. Successful synthesis of **3b** was achieved after adopting the methodology published by Polanc [16] through diketonatoboron difluoride **4a**.

2.2. X-ray study

The compound **5a** (Fig. 1) crystallizes in the monoclinic crystal system with *P*21/*c* space group with four molecules within the unit cell and compound **5b** (Fig. 2) crystallizes in the orthorhombic crystal system with *Pbca* space group with eight molecules within the unit cell. In both compounds no intramolecular or intermolecular contacts are present.

The boron atom in compound **5a** lies out of the heteroatomic ring plane (the torsion of 38.98(3)° (Fig. 3) where the rest of the atoms forming this six-membered ring are involved in a π-electron conjugated system. The boron atom has the geometry of a distorted tetrahedron. The interatomic distances of B—O (1.508 Å) and B—N (1.579 Å) in **5a** are comparable to the previously reported structurally related species [11–14]. In boron diketonates, the B—O distances are comparable with those in **5a**, on the other hand, in the molecule where boron atom is substituted by two fluoride atoms, the B—O bond is much shorter (1.466 Å) [17–19].

In the compound **5b** the formation of the planar arrangement of the O—C3—N atoms is suppressed probably by steric as well as

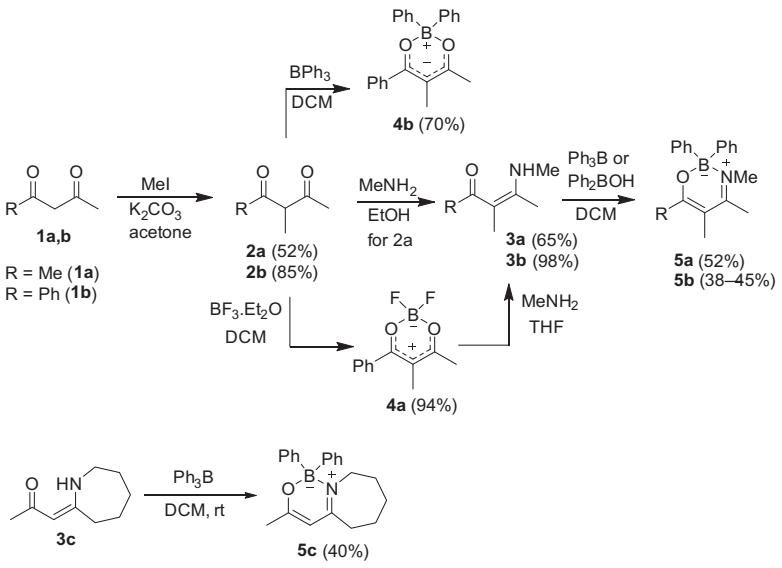

Scheme 2. Synthesis of the boron heterocycles.

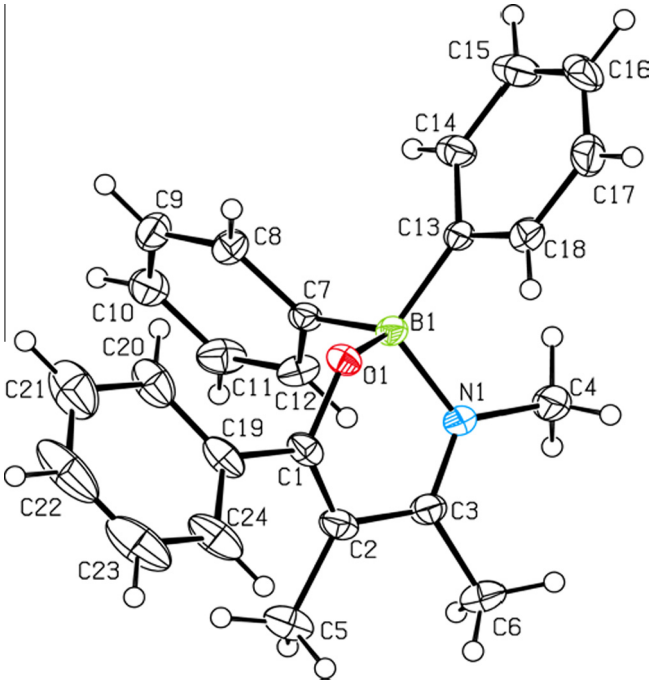

Fig. 2. The molecular structure (ORTEP 40% probability level) of **5b**.

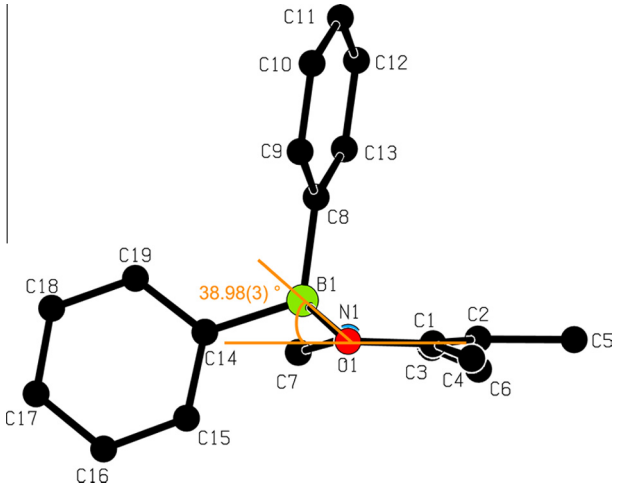

Fig. 3. Angle between O1—B1—N1 plane and the rest of heteroatomic ring O1—C1—C2—C3—N1 in compound **5a**.

electronic influence of the phenyl substituent at the C1 atom instead of the methyl substituent in **5a**, O1 and N1 are thus located slightly out of the C1—C2—C3 plane. Other interatomic distances and angles are comparable to the corresponding parameters found in **5a**.

2.3. NMR Study

All boron chelates were characterized by their ^{11}B chemical shifts. Boron signal of difluoroboron diketonate **4a** should be, in principle, split to triplet. In reality, the signal of **4a** is a broad singlet. Gardinier et al. [18] explained this observation by quadrupolar effect of the boron and by a magnetic anisotropy of the chelate ring. Boron-11 chemical shift of **4a** ($\delta = 0.18$) lies in the area typical for four-coordinated BF_2 compounds (Gardinier observed chemical shifts for difluoroboron diaryldiketonates in range 0.23–0.99 ppm). Fluorine-19 NMR spectrum of **4a** consists of two broad singlets ($^{10}BF_2$ and $^{11}BF_2$) whose chemical shifts (ca −142 ppm) are also comparable with those described by Gardinier. In comparison with fluorine-19 chemical shifts of difluoroboron ketoiminates e.g. [17,18], β-diketonates possess certain upfield shift, which is explained by the anisotropy of the chelate ring of the diketonate causing greater shielding of the fluorines than in the ketoiminates [18].

The substitution of the fluorines in **4a** for phenyls leads to a downfield shift in ^{11}B NMR of **4b** (0.18 ppm for **4a** vs. 7.56 ppm for **4b**). This effect is common [20]. The chemical shift of **4b** is comparable with those published e.g. by Chujo et al. [21].

Boron chemical shifts of diphenylboron ketoiminates **5** (3.54 and 3.76 ppm resp.) are more upfielded than those of *N*-coumarin-6-yl substituted oxazaborines ([17], $\delta = 4.9–5.5$) which can be caused e.g. by lower steric effect of the *N*-methyl group in comparison with the coumarin-6-yl fragment. Greater degree of conjugation then cause larger shielding of the boron atom leading to the observed upfield shift. An electron-donating effect of the C4 methyl group can also play a role in the increased shielding of the boron atom in **5**.

2.4. Electrochemical data and quantum chemical correlations

The studied compounds within the series were selected in such a manner enabling direct comparison of the electrochemical data of at least two compounds differing only in one feature. In this way the influence of individual structural motifs can be followed. Experimental data of the first oxidation and the first reduction potential, wavelengths of main bands in UV–Vis spectra and calculated HOMO and LUMO energies are presented in the Table 1. The calculated distribution of HOMO and LUMO orbitals, respectively, is depicted in the Fig. 4.

To interconnect the previous and the present series of compounds, the oxazaborine **6** [15b] was taken for direct comparison with its homologue **5c**. The phenylazo-pendant in compound **6** represents a conjugated system extending the electron delocalization of the heterocycle. In the absence of the phenylazo substituent (**5c**) the oxidation and reduction centers are located at the boron heterocycle: HOMO involves mostly the negatively charged boron atom, the other two heteroatoms and at the opposite C5—C6 bond of the heterocycle, LUMO is located at the O—C and N=C bonds of the heterocycle (cf. Fig. 4). On the other hand, oxidation of **6** as well as reduction of **6** proceeds more

Table 1
Experimental data of the first oxidation and the first reduction potential, compared with calculated HOMO and LUMO energies.

Compound	$E_{1/2}$ (ox 1) [V]	$E_{1/2}$ (red 1) [V]	ΔE[d] [V]	E_{HOMO} calculated (eV)	E_{LUMO} calculated (eV)	HOMO-LUMO gap
4a	–	−1.14[b]		−7.02	−2.66	4.36
4b	–	−1.31[b]		−6.54	−2.46	4.08
5a	1.29[a]	−2.25 (85 mV[c])	3.51	−5.94	−1.48	4.46
5b	1.34[b]	−1.89[b]	3.23	−5.96	−1.90	4.06
5c	1.50[a]	−2.21 (78 mV[c])	3.63	−6.14	−1.62	4.52
6	1.27[b]	−1.58[b]	2.85	−6.00	−2.20	3.80

All potentials are given vs. SCE.
[a] Potential of the irreversible anodic peak (E_{pa}) taken from cyclic voltammetry at Pt-electrode.
[b] Half-wave potential ($E_{1/2}$) taken from voltammetry at a platinum rotating disk electrode (RDE).
[c] Half-wave potential ($E_{1/2}$) taken from reversible cyclic voltammogram as average value of oxidation and reduction peak potential, respectively ($E_{pc} - E_{pa}/2$).
[d] Difference between the first oxidation and reduction potentials.

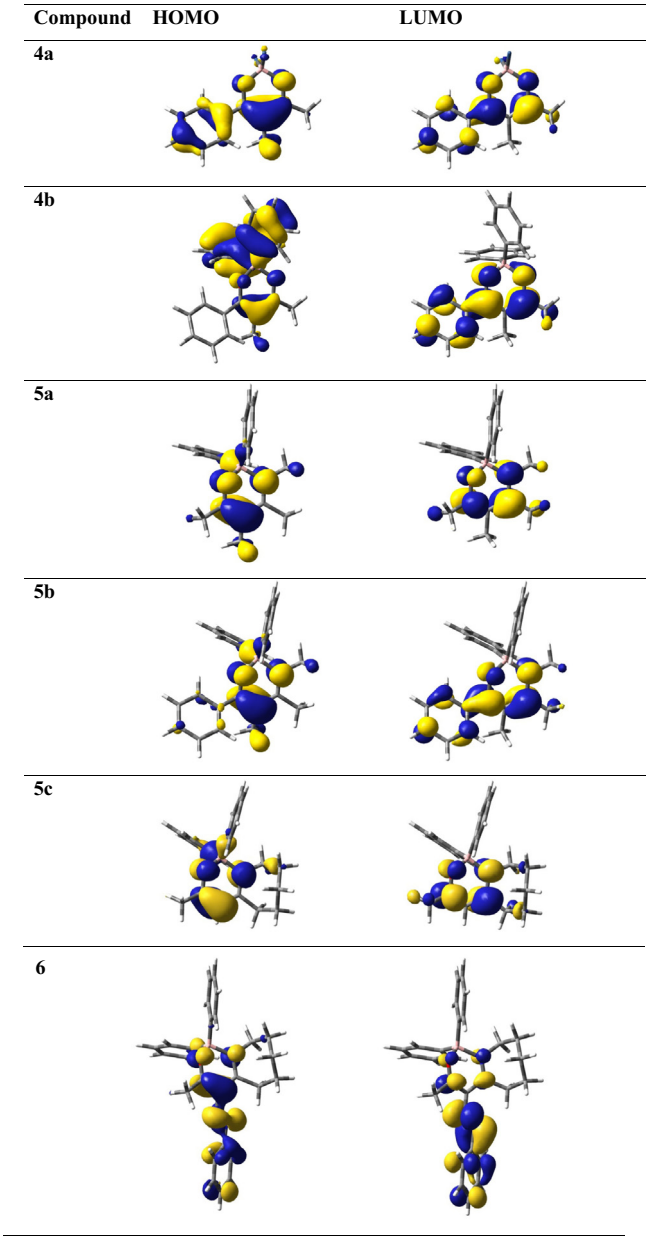

Fig. 4. Calculated distribution of HOMO and LUMO in molecules under study.

easily with respect to **5c**, hence at "lower" (in absolute values) potentials. The maps of LUMO and HOMO orbitals of **6** show that the reduction center involves the azo group and the oxidation occurs partly at the phenylazo-pendant, too. The limited π-electron system in **5c** results in more positive oxidation potential and more negative reduction potential, that means in larger gap between E_{ox} and E_{rec} in comparison with **6**.

For comparison of **5c** and **5a**, one should accept a legitimate approximation, that the saturated [3,4-*a*]azepine ring would be electronically similar to the two methyl groups in positions 3 and 4. Then the only significant difference is the 5-methyl group in **5a**. The above mentioned approximation is confirmed by very close reduction potentials of both derivatives (see Table 1), where the 5-methyl compound **5a** has the reduction potential only by 40 mV more negative (according to expectations) than **5c**. On the other hand, the 5-methyl substituent in **5a** is directly connected with the HOMO at the C5—C6 bond. Therefore, the oxidation potential of **5a** is shifted by 210 mV less positively compared to **5c** reflecting the donor character of the methyl group making the oxidation easier.

The compounds **5a** and **5b** differ only in the substitution at the position 6: The methyl derivative **5a** is oxidized by 50 mV less positively (according to expectations) in comparison with the phenyl derivative **5b**. On the other hand, the reduction potential of **5a** is significantly (by 360 mV) more negative than that of **5b**. The reason of such an easy reduction of **5b** is the extended π-delocalized system involving also the phenyl ring in the position 6 (cf. maps of HOMO and LUMO orbitals at the Fig. 4).

The derivatives **4b** and **5b** structurally interconnect the boron diketonates and ketoiminates, where the heteroatom oxygen is replaced by the positively charged quarternary iminium group substituted by an additional methyl. As a result, the boron ketoiminate **5b** is more easily oxidized but more hardly reduced (the iminium methyl group here plays a role) in comparison with analogous diketonate **4b**. However, due to different charge distribution in the two types of heterocycles, a deeper discussion is difficult.

In the case of diketonates, the replacement of two phenyl rings in the position 2 of the boron diketonate **4b** by two fluorine atoms results in less negative reduction of the compound **4a** by 170 mV due to the electron-withdrawing effect of the two fluorine atoms. Oxidation potentials of these two diketonates are out of the accessible potential range and therefore they could not be determined. The totally different location of HOMOs (cf. Fig. 4) is very noteworthy, especially that of **4b**, which is located exclusively on the BPh_2 part of the molecule.

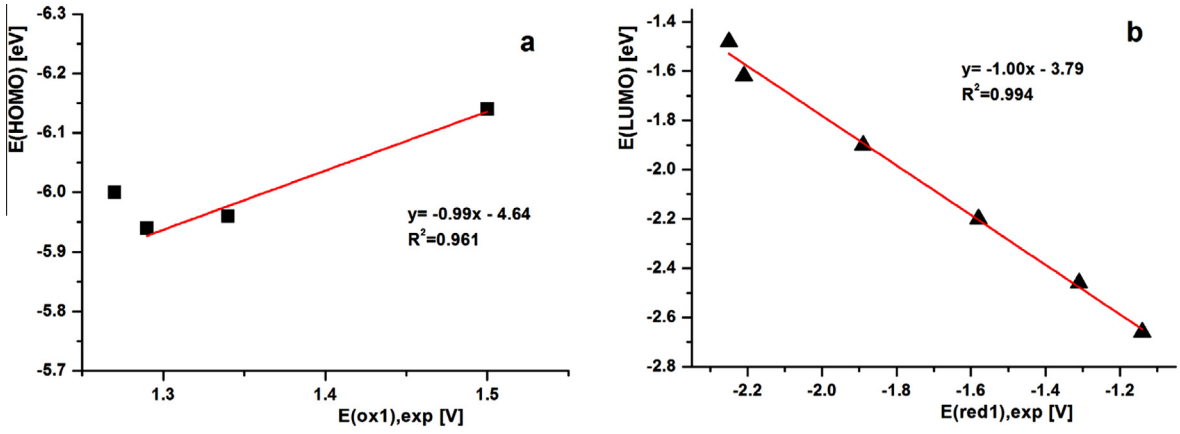

Fig. 5. Correlation of a) the measured first oxidation potentials with calculated HOMO energies and b) the measured first reduction potentials with calculated LUMO energies.

Please cite this article in press as: T. Mikysek et al., Inorg. Chim. Acta (2016), http://dx.doi.org/10.1016/j.ica.2016.08.009

From the Table 1 it is evident that the difference between the first oxidation and the first reduction potentials correlates well with calculated HOMO-LUMO gap. Similarly, the measured first oxidation potentials correlate with calculated HOMO energies and the measured first reduction potentials correlate with calculated LUMO energies (Fig. 5a and b), both with the slope close to unity, confirming the appropriateness of the experimental as well as theoretical approach. Similar good correlation offer the plots of experimental versus calculated values of the first oxidation and reduction potentials, respectively.

2.5. UV–Vis spectra and quantum chemical correlations

Optical properties of the title compounds were investigated by the absorption electron spectra measured in acetonitrile in the UV–Vis region (Fig. 6). The measured wavelengths of absorption maxima and their corresponding energies in eV are summarized in the Table 2 together with calculated values yielding a good correlation (Fig. 7). The longest-wavelength absorption bands with λ_{max} between 330 and 362 nm are dominating in the obtained spectra.

The HOMO-LUMO transitions of the compounds **4a**, **4b**, **5a**, **5b** and **5c** correspond to the pure lowest π-π^* transition on heterocyclic ring. The observed spectra are of rather low intensity which correlates with the Oscillator Strength values (dimensionless quantity which is proportional to the integral intensity of the corresponding absorption band and points to the intensity of the transition). These values presented in the Table 2 fit well with the intensities of the corresponding experimental spectra. The most intensive one belongs to the di-fluorinated diketonate **4a**, where HOMO is located at the phenyl ring attached to the heterocycle as distinct from the similar structures **4b** and **5b** (cf. Fig. 4). The compound **6** has the second most intensive band (within the studied compounds) where several transitions contribute (see Table 2) most probably thanks to the azo pendant.

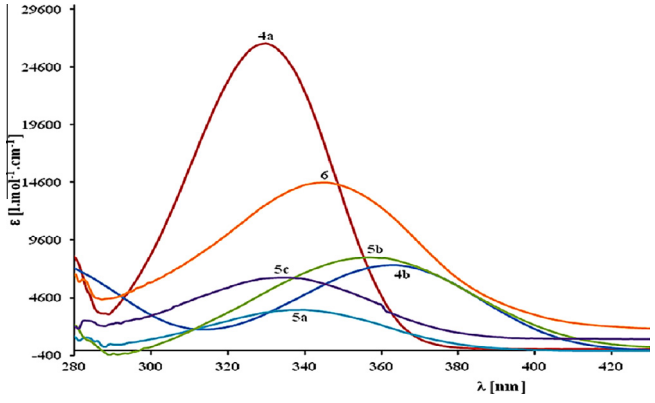

Fig. 6. UV–Vis absorption spectra of OZB and OOB compounds measured in acetonitrile.

Table 2
Quantum-chemical calculations of electron transitions.

Compound	λ_{max} experim. [nm] (eV)	λ_{max} calculated [nm]	Oscillator strength	Orbital transition (% contribution)
4a	330 (3.76)	313	0.533	HOMO → LUMO (98)
4b	362 (3.43)	359	0.0166	HOMO → LUMO (94)
5a	338 (3.67)	318	0.120	HOMO → LUMO (98)
5b	353 (3.51)	354	0.230	HOMO → LUMO (99)
5c	334 (3.71)	317	0.128	HOMO → LUMO (97)
6	345 (3.59)	356	0.652	HOMO → LUMO (43) HOMO−1 → LUMO (30) HOMO → LUMO+1 (25)

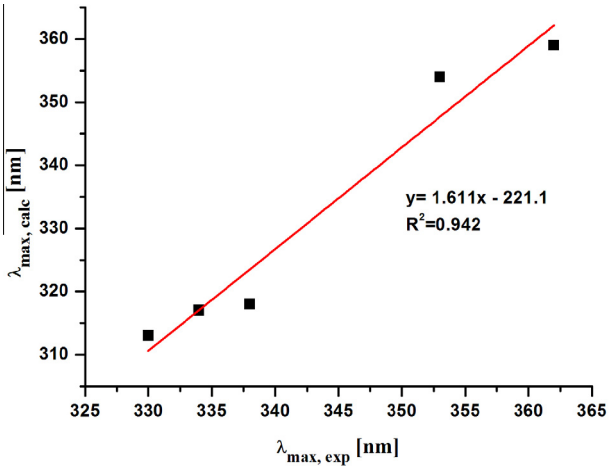

Fig. 7. Correlation of the measured λ_{max} with the calculated λ_{max} (from the Table 2).

3. Conclusions

A series of three new oxazaborine and two boron diketonate derivatives containing different structural motifs were synthesized and characterized using NMR, UV–Vis spectra and X-ray structure analysis. Their oxidation and reduction abilities were investigated electrochemically using rotating-disk voltammetry, cyclic voltammetry and dc-polarography. The experiments were focused mainly to the first oxidation and first reduction potential, since their values are related to HOMO and LUMO energies.

For understanding of the relationship between the structure and redox properties, the electronic influence of individual substituents on the reduction and oxidation potential was followed. Whereas the oxazaborines **5a**–**c** are reduced very negatively (−1.89 to −2.25 V vs. SCE), the reduction potentials of boron diketonates are about 800 mV less negative. However, the opposite situation is in oxidation: oxazaborines are oxidized at 1.29–1.50 V vs. SCE, whereas oxidation of boron diketonates does not proceed within the accessible potential range.

Using DFT method, the energies of HOMO and LUMO together with the reduction and oxidation potentials were calculated and compared with experimental values. The good correlation confirms the credibility and reliability of experimental as well as theoretical approach. Similarly, the energies of the longest-wavelength absorption bands taken from UV–Vis spectra were compared with the experimentally found differences E_{ox}–E_{red} and with calculated HOMO-LUMO gaps and transition energies.

4. Experimental

4.1. Electrochemistry

Electrochemical measurements were carried out in *N*,*N*-dimethylformamide containing 0.1 M Bu_4NPF_6. DC polarography, cyclic voltammetry (CV) and rotating disk voltammetry (RDV) were used in a three electrode arrangement. The working electrode was dropping mercury electrode (DME) for polarographic measurements (drop time τ_D = 1 s, scan rate υ = 5 mV.s^{-1}), hanging mercury drop electrode (HMDE) for CV and platinum or glassy carbon disk (2 mm in diameter) for oxidation and RDV experiments. As the reference and auxiliary electrodes were used saturated calomel electrode (SCE) separated by a bridge filled with supporting

electrolyte and a Pt wire, respectively. All potentials are given vs. SCE. Voltammetric measurements were performed using a potentiostat PGSTAT 128 N (AUTOLAB, Metrohm Autolab B.V., Utrecht, The Netherlands) operated via NOVA 1.11 software.

4.2. Crystallography

The X-ray data for colorless crystals of **5a** and yellow of **5b** ware obtained at 150 K using Oxford Cryostream low-temperature device on a Nonius KappaCCD diffractometer with Mo K_α radiation (λ = 0.71073 Å), a graphite monochromator, and the ϕ and χ scan mode. Data reductions were performed with DENZO-SMN [22]. The absorption was corrected by integration methods [23]. Structures were solved by direct methods (Sir92) [24] and refined by full matrix least-square based on F^2 (SHELXL97) [25]. Hydrogen atoms were mostly localized on a difference Fourier map, however to ensure uniformity of treatment of crystal, all hydrogen were recalculated into idealized positions (riding model) and assigned temperature factors $H_{iso}(H) = 1.2\ U_{eq}$ (pivot atom) or of $1.5\ U_{eq}$ (methyl). H atoms in methyl moieties and hydrogen atoms in aromatic rings were placed with C—H distances of 0.96 and 0.93 Å.

$R_{int} = \Sigma|F_o^2 - F_{o,mean}^2|/\Sigma F_o^2$, GOF = $[\Sigma(w(F_o^2 - F_c^2)^2)/(N_{diffrs} - N_{params})]''$ for all data, $R(F) = \Sigma||F_o| - |F_c||/\Sigma|F_o|$ for observed data, $wR(F^2) = [\Sigma(w(F_o^2 - F_c^2)^2)/(\Sigma w(F_o^2)^2)]''$ for all data.

Crystallographic data for structural analysis have been deposited with the Cambridge Crystallographic Data Centre, CCDC No. 1454995 and 1454996 for **5a** and **5b**. Copies of this information may be obtained free of charge from the Director, CCDC, 12 Union Road, Cambridge CB2 1EY, UK (fax: +44-1223-336033; e-mail: deposit@ccdc.cam.ac.uk or www: http://www.ccdc.cam.ac.uk).

4.3. NMR and UV–Vis spectroscopy and other instrumentation

NMR Spectra were measured in $CDCl_3$ using either Bruker AVANCE III operating at 400.13 MHz (^{1}H), 100.61 MHz (^{13}C), 376.50 MHz (^{19}F) and 128.38 MHz (^{11}B) or Bruker Ascend™ operating at 500.20 MHz (^{1}H), 125.78 MHz (^{13}C), 470.66 MHz (^{19}F) and 160.48 MHz (^{11}B). Proton NMR spectra were calibrated on an internal TMS (δ = 0.00), carbon spectra on the middle signal of the solvent multiplet (δ = 77.23), fluorine spectra on α,α,α-trifluorotoluene (δ = −63.9) and boron spectra on trimethoxyborane (δ = 18.1). Boron-11 NMR spectra were measured in 5 mm quartz NMR tubes (Norell). Both carbon and fluorine spectra were measured under proton decoupling. UV–Vis spectra were recorded on a Shimadzu UV-2450 spectrophotometer in acetonitrile. Elemental analyses were performed on a Flash EA 2000 CHNS automatic analyser (Thermo Fisher Scientific). HRMS were measured on a MALDI LTQ Orbitrap XL (Thermo Fisher Scientific).

4.4. Quantum chemical calculations

Structures of the studied molecules were calculated using the density functional theory (DFT) method with Becke's three-parameter hybrid functional B3LYP [26,27] and triple-ζ polarized 6-311G (d) [28] basis sets for all atoms. Geometries of all the compounds were fully optimized with no symmetry constraints. Vibrational analyses followed on the optimized structures to ensure proper character of the stationary states. Electronic transitions were calculated on the ground-state optimized structures with aid of the time-dependent DFT (TDDFT) method [29]. Gaussian 09 software package (G09) [30] was used for all the calculations. The effect of solvation was accounted for by the polarizable continuum model (PCM) [31,32] with solvent parameters according to the experiments, as implemented in the G09 using the integral equation formalism [33]. Maps of the frontier molecular orbitals were plotted using the GaussView software.

4.5. Synthesis

All the solvents and reagents were commercial and used without further treatment. Dry solvents were stored under argon using AcroSeal™ or Sure/Seal™ technology.

5. General procedure for *C*-methylation of β-diketones

Appropriate β-diketone (100 mmol) was dissolved in anhydrous acetone (80 mL). Subsequently, anhydrous potassium carbonate (93 mmol) was added under inert. After stirring the solution for 5 min. at room temperature, methyl iodide (7.72 mL, 100 mmol) was added dropwise during 10 min. The reaction mixture was then refluxed for 12 h. Volatile components were distilled off, the residue was diluted with ether (100 mL) and precipitated solid was removed by suction. The filtrate was evaporated in vacuo and the residue was further purified.

5.1. 2-Methylacetylacetone (*2a*)

Prepared from acetylacetone. Purification through its copper diketonate using the methodology published e.g. in [34]. Yield 52% of yellow-brown liquid. In $CDCl_3$ the product is 3:2 mixture of enol-keto tautomers. ^{1}H NMR (400 MHz, $CDCl_3$): keto form δ = 3.71 (q, J = 7.1 Hz, 1H), 2.20 (s, 6H), 1.33 (d, J = 7.1 Hz, 3H); enol form δ = 16.46 (s, 1H), 2.12 (s, 6H), 1.85 (s, 3H). Data are in accordance with those published in [35].

5.2. 2-Methylbenzoylacetone (*2b*)

Prepared from benzoylacetone. Purification by a column chromatography (hexane/EtOAc, 8:1 v/v). Yield 85% of yellow liquid. The product is almost pure keto form in $CDCl_3$. ^{1}H NMR (400 MHz, $CDCl_3$) δ = 7.99–7.97 (m, 2H), 7.62–7.58 (m, 1H), 7.52–7.48 (m, 2H), 4.50 (q, J = 7.0 Hz, 1H), 2.17 (s, 3H), 1.46 (d, J = 7.0 Hz, 3H) ppm. The data are in accordance with those published in [36].

5.3. 3-Methyl-4-methylaminopent-3-en-2-one (*3a*)

The mixture of β-diketone **2a** (22 mmol, 2.46 g) in EtOH (41 mL) and Me_2NH (33 wt% solution in EtOH; 0.2 mol Me_2NH) was refluxed for 5 h. The volatile components were evaporated in vacuo and the residue was separated between DCM (50 mL) and water (50 mL). Organic layer was dried over Na_2SO_4 and evaporated under reduced pressure to give oily product. Yield: 1.78 g, 65%. ^{1}H NMR (400 MHz, $CDCl_3$): δ = 11.86 (br s, 1H), 2.94 (d, J = 5.1 Hz, 3H), 2.13 (s, 3H), 1.97 (s, 3H), 1.84 (s, 3H).

5.4. 2-Methyl-3-(methylamino)-1-phenylbut-2-en-1-one (*3b*)

To a stirred solution of a boron complex **4a** (3.59 g, 16 mmol) in anhydrous acetonitrile (15 mL), methylamine solution in THF (8.4 mL, 48 mmol) was added. The reaction mixture was stirred at room temperature for 1.5 h and volatile components were then evaporated. The residue was dissolved in dichloromethane (50 mL), washed with water (2 × 25 mL), dried over anhydrous sodium sulfate and evaporated to dryness. Yield 2.97 g (98%) of red solid with mp 59.5–61 °C (Ref. [37] gives 70–71 °C). ^{1}H NMR (400 MHz, $CDCl_3$): δ = 12.44 (br s, 1H), 7.31–7.39 (m, 5H), 3.04 (d, J = 5.3 Hz, 3H), 2.07 (s, 3H) 1.82 (s, 3H) ppm. ^{13}C NMR (100 MHz, $CDCl_3$): δ = 192.4, 166.5, 143.3, 128.2, 127.8, 126.9, 97.6, 30.1, 16.4, 15.5 ppm.

5.5. 2,2-Difluoro-4,5-dimethyl-6-phenyl-1,3,2λ^4-dioxaborine (**4a**)

The method was adopted from [16]. To a solution of 1,3-diketone **2b** (3 g, 17 mmol) in dichloromethane (45 mL), boron trifluoride etherate (6.43 mL, 51 mmol) was added at room temperature. The reaction mixture was stirred at room temperature for 25 h. Afterwards, volatile components were evaporated and the residue was suspended in water (60 mL). Solid material was filtered off and dried in a vacuum furnace. Yield: 3.59 g (94%) of yellow solid. The sample for electrochemical study was further recrystallized from ethanol to give white solid with mp 76–77 °C (Ref. [38] reports 153–154 °C). ^{1}H NMR (400 MHz, $CDCl_3$): δ = 7.72–7.69 (m, 2H), 7.61–7.57 (m, 1H), 7.52–7.48 (m, 2H), 2.46 (s, 3H), 2.10 (s, 3H) ppm. ^{13}C NMR (100 MHz, $CDCl_3$): δ = 194.3, 184.1, 133.5, 133.1, 129.9, 128.7, 24.0, 14.2 ppm. ^{19}F NMR (376.5 MHz, $CDCl_3$): δ = −142.06 ($^{10}BF_2$), −142.13 ($^{11}BF_2$) ppm. ^{11}B NMR (160.5 MHz, $CDCl_3$) δ = 0.18 ppm. HRMS for $C_{11}H_{11}BF_2O_2$ calc. $[M-F]^+$ 205.08307 $[M+Na]^+$ 247.07124 $[M+K]^+$ 263.04518 $[2M+Na]^+$ 471.15271, found $[M-F]^+$ 205.08322 $[M+Na]^+$ 247.07143 $[M+K]^+$ 263.04540 $[2M+Na]^+$ 471.15373.

5.6. 4,5-Dimethyl-2,2,6-triphenyl-1,3,2λ^4-dioxaborine (**4b**)

The flask fitted with a calcium-chloride drying tube was charged with 1,3-diketone **2b** (1 g, 5.7 mmol) in anhydrous DCM (25 mL). Afterwards BPh_3 (1.65 g, 6.8 mmol) was added in one portion. The reaction mixture was stirred for 4 days at laboratory temperature and then concentrated under reduced pressure. The residue was recrystallized from ethanol. Yield: 1.35 g (70%) of yellow solid, mp 107–108 °C. ^{1}H NMR (500 MHz, $CDCl_3$): δ = 7.70–7.73 (m, 2H), 7.51–7.54 (m, 5H), 7.44–7.48 (m, 2H), 7.26–7.29 (m, 4H), 7.18–7.22 (m, 2H), 2.38 (s, 3H), 1.91 (s, 3H) ppm. ^{13}C NMR (125 MHz, $CDCl_3$): δ = 193.4, 183.2, 148.1 (br), 134.8, 132.3, 131.5, 129.7, 128.5, 127.4, 126.6, 107.3, 24.0, 14.6 ppm. ^{11}B NMR (160.5 MHz, $CDCl_3$) δ = 7.56 ppm. Found C, 81.21; H, 6.27. $C_{23}H_{21}BO_2$ requires C, 81.20; H, 6.22.

5.7. Synthesis of oxazaborines **5**

5.7.1. Method A

The flask fitted with a calcium-chloride drying tube was charged with enaminone **3** in anhydrous DCM (8 mL/mmol). Afterwards diphenylborinic acid (2 eq.) was added gradually under stream of argon. The reaction mixture was stirred for 5 days at laboratory temperature and then concentrated under reduced pressure. The residue was purified.

5.7.2. Method B

The flask fitted with a calcium-chloride drying tube was charged with enaminone **3** in anhydrous DCM (8 mL/mmol). Afterwards BPh_3 (1.1–2 eq.) was added gradually under stream of argon during 30 min. The reaction mixture was stirred 1–5 days at laboratory temperature and then concentrated under reduced pressure. The residue was purified.

5.8. 3,4,5,6-Tetramethyl-2,2-diphenyl-[1,3,2-λ^4]oxazaborine (**5a**)

Prepared using method B, 1.1 eq. BPh_3, reaction time 3 days, purification by a column chromatography (silica gel/DCM). Yield 52%, mp 93.5–94 °C. ^{1}H NMR (400 MHz, $CDCl_3$): δ = 7.32–7.30 (m, 4H), 7.27–7.18 (m, 6H), 2.92 (s, 3H), 2.13 (s, 3H), 2.04 (s, 3H), 1.75 (s, 3H); ^{13}C NMR (100 MHz, $CDCl_3$): δ = 171.7, 169.2, 133.1, 127.2, 126.2, 102.9, 38.3, 21.5, 17.3, 14.1 ppm. ^{11}B NMR (160.5 MHz, $CDCl_3$) δ = 3.54 ppm. Found C, 78.29; H, 7.53; N, 4.78. $C_{19}H_{22}BNO$ requires C, 78.37; H, 7.62; N, 4.81.

Crystallographic data for **5a**: $C_{19}H_{22}BNO$, M = 291.19, monoclinic, $P21/c$, a = 8.3370(5) Å, b = 10.0640(9) Å, c = 19.8901(14) Å, β = 94.256(6) °, Z = 4, V = 1664.3(2) Å^3, D_c = 1.162 g.cm^{-3}, μ = 0.070 mm^{-1}, T_{min}/T_{max} = 0.981/0.988; $-10 \leqslant h \leqslant 10$, $-12 \leqslant k \leqslant 13$, $-23 \leqslant l \leqslant 25$; 13938 reflections measured (θ_{max} = 27.49°), 3760 independent (R_{int} = 0.0279), 3066 with $I > 2\sigma(I)$, 199 parameters, S = 1.070, $R1$(obs. data) = 0.0467, w$R2$ (all data) = 0.1143; max., min. residual electron density = 0.286, −0.317 eÅ^{-3}.

5.9. 3,4,5-Trimethyl-2,2,6-triphenyl-1,3,2λ^4-oxazaborine (**5b**)

Method A, reaction time 5 days, purification by means of column chromatography (silica gel, DCM) followed by recrystallization from ethanol, yield 38%. Method B: 1.5 eq. BPh_3, reaction time 5 days, purification by means of column chromatography (silica gel, DCM), yield 45%.

Bright yellow solid, mp 167–167.5 °C. ^{1}H NMR (400 MHz, $CDCl_3$): δ = 7.52–7.50 (m, 2H), 7.38–7.34 (m, 7H), 7.25–7.20 (m, 6H), 2.96 (s, 3H), 2.27 (s, 3H), 1.86 (s, 3H) ppm. ^{13}C NMR (100 MHz, $CDCl_3$): δ = 171.7, 169.2, 133.0, 131.4, 127.1, 126.2, 102.8, 38.2, 21.4, 17.2, 14.0 ppm. ^{11}B NMR (160.5 MHz, $CDCl_3$): δ = 3.76 ppm. Found C, 81.60; H, 6.87; N, 3.89. $C_{24}H_{24}BNO$ requires C, 81.60; H, 6.85; N, 3.96.

Crystallographic data for **5b**: $C_{24}H_{24}BNO$, M = 353.25, orthorhombic, $Pbca$, a = 10.7690(14) Å, b = 14.2530(12) Å, c = 25.563(3) Å, β = 90°, Z = 8, V = 3923.7(8) Å^3, D_c = 1.196 g.cm^{-3}, μ = 0.071 mm^{-1}, T_{min}/T_{max} = 0.981/0.987; $-13 \leqslant h \leqslant 11$, $-18 \leqslant k \leqslant 18$, $-33 \leqslant l \leqslant 30$; 20639 reflections measured (θ_{max} = 27.50°), 4452 independent (R_{int} = 0.0438), 3202 with $I > 2\sigma(I)$, 244 parameters, S = 1.092, $R1$(obs. data) = 0.0579, w$R2$ (all data) = 0.1189; max., min. residual electron density = 0.250, −0.257 eÅ^{-3}.

5.10. 3-Methyl-1,1-diphenyl-6,7,8,9-tetrahydro-5H-[1,3,2-λ^4] oxazaborino[3,4-a]azepine (**5c**)

Method B, gradual addition of BPh_3 under cooling (5 °C), reaction time 24 h, purification by column chromatography (silica gel, DCM). Yield 40% of white solid, mp 210.5–211.5 °C. ^{1}H NMR (400 MHz, $CDCl_3$): δ = 7.38–7.36 (m, 4H), 7.28–7.24 (m, 4H), 7.23–7.19 (m, 2H), 5.11 (s, 1H, =CH), 3.44–3.41 (m, 2H), 2.50–2.47 (m, 2H), 2.00 (s, 3H, CH_3), 1.68–1.63 (m, 4H), 1.22–1.18 (m, 2H). ^{13}C NMR (100 MHz, $CDCl_3$): δ = 176.7, 173.8, 149.4 (br), 133.1, 127.1, 126.3, 98.6 (=CH), 50.3, 35.7, 30.1, 26.8, 24.0, 23.2 ppm. ^{11}B NMR (117.5 MHz, $CDCl_3$): δ = 4.75 ppm. Found C, 79.56; H, 7.63; N, 4.31. $C_{21}H_{24}BNO$ requires C, 79.51; H, 7.63; N, 4.42.

Acknowledgements

The authors H.K. and J.L. are grateful to the institutional support RVO 61388955.

H.K. is further indebted to the Ministry of Education of the Czech Republic (grant LD14129).

Appendix A. Supplementary data

Supplementary data associated with this article can be found, in the online version, at http://dx.doi.org/10.1016/j.ica.2016.08.009.

References

[1] M.J.S. Dewar, V.P. Kubba, R. Pettit, J. Chem. Soc. (1958) 3073.
[2] M.J.S. Dewar, V.P. Kubba, R. Pettit, J. Chem. Soc. (1958) 3076.
[3] M.J.S. Dewar, R. Dietz, J. Chem. Soc. (1958) 27.

[4] M.J.D. Bosdet, W.E. Piers, Can. J. Chem. 86 (2009) 8.
[5] C.D. Entwistle, T.B. Marder, Angew. Chem. Int. Ed. 41 (2002) 2927.
[6] C.D. Entwistle, T.B. Marder, Chem. Mater. 16 (2004) 4574.
[7] A. Loudet, R. Bandichhor, L.X. Wu, K. Burgess, Tetrahedron 64 (2008) 3642.
[8] H.Y. Chen, Y. Chi, C.S. Liu, J.K. Yu, Y.M. Cheng, K.S. Chen, P.T. Chou, S.M. Peng, G. H. Lee, A.J. Carty, S.J. Yeh, C.T. Chen, Adv. Funct. Mater. 15 (2005) 567.
[9] A.H. Soloway, W. Tjarks, B.A. Barnum, F.G. Rong, R.F. Barth, I.M. Codogni, J.G. Wilson, Chem. Rev. 98 (1998) 1515.
[10] M.A. Grassberger, F. Furnowsky, J. Hildebrant, J. Med. Chem. 27 (1984) 947.
[11] M. Pešková, P. Šimůnek, V. Bertolasi, V. Macháček, A. Lyčka, Organometallics 25 (2006) 2025.
[12] M. Svobodová, J. Bárta, P. Šimůnek, V. Bertolasi, V. Macháček, J. Organomet. Chem. 694 (2009) 63.
[13] M. Svobodová, P. Šimůnek, V. Macháček, L. Štruncová, A. Růžička, Tetrahedron 68 (2012) 2052.
[14] F. Josefík, M. Svobodová, V. Bertolasi, P. Šimůnek, V. Macháček, N. Almonasy, E. Černošková, J. Organomet. Chem. 699 (2012) 75.
[15] (a) F. Josefík, T. Mikysek, M. Svobodová, P. Šimůnek, H. Kvapilová, J. Ludvík, Organometallics 33 (2014) 4931;
(b) T. Mikysek, H. Kvapilová, F. Josefík, J. Ludvík, Anal. Lett. 49 (2016) 178.
[16] B. Štefane, S. Polanc, New J. Chem. 26 (2002) 28.
[17] H. Doušová, P. Šimůnek, N. Almonasy, Z. Růžičková, J. Organomet. Chem. 802 (2016) 60.
[18] F.P. Macedo, C. Gwengo, S.V. Lindeman, M.D. Smith, J.R. Gardinier, Eur. J. Inorg. Chem. (2008) 3200.
[19] K. Itoh, K. Okazaki, M. Fujimoto, Aust. J. Chem. 56 (2003) 1209.
[20] G.R. Eaton, J. Chem. Educ. 46 (1969) 547.
[21] A. Nagai, K. Kokado, Y. Nagata, M. Arita, Y. Chujo, J. Org. Chem. 73 (2008) 8605.
[22] Z. Otwinowski, W. Minor, Processing of X-ray diffraction data collected in oscillation mode, in: C.W. Carter, R.M. Sweet (Eds.), Methods in Enzymology, vol. 276, 1997, p. 307. London.
[23] P. Coppens, in: F.R. Ahmed, S.R. Hall, C.P. Huber (Eds.), Crystallographic Computing, Munksgaard, Copenhagen, 1970, p. 255.
[24] A. Altomare, G. Cascarano, C. Giacovazzo, A. Guagliardi, J. Appl. Crystallogr. 27 (1994) 1045.
[25] G.M. Sheldrick, SHELXL-97, University of Göttingen, Göttingen, 2008.
[26] C.T. Lee, W.T. Yang, R.G. Parr, Phys. Rev. B 37 (1988) 785.
[27] A.D. Becke, J. Chem. Phys. 98 (1993) 5648.
[28] R. Krishnan, J.S. Binkley, R. Seeger, J.A. Pople, J. Chem. Phys. 72 (1980) 650.
[29] M.E. Casida, in: D.P. Chong (Ed.), Recent Advances in Density Functional Methods, World Scientific, Singapore, 1995, p. 155.
[30] M.J. Frisch, G.W. Trucks, H.B. Schlegel, G.E. Scuseria, M.A. Robb, J.R. Cheeseman, G. Scalmani, V. Barone, B. Mennucci, G.A. Petersson, H. Nakatsuji, M. Caricato, X. Li, H.R. Hratchian, A.F. Izmaylov, J. Bloino, G. Zheng, J.L. Sonnenberg, M. Hada, M. Ehara, K. Toyota, R. Fukuda, J. Hasegawa, M. Ishida, T. Nakajima, Y. Honda, O. Kitao, H. Nakai, T. Vreven, J.A. Montgomery Jr., J.R. Peralta, F. Ogliaro, M. Bearpark, J.J. Heyd, E. Brothers, K.N. Kudin, V.N. Staroverov, R. Kobayashi, J. Normand, K. Raghavachari, A. Rendell, J.C. Burant, S.S. Iyengar, J. Tomasi, M. Cossi, N. Rega, J.M. Millam, M. Klene, J.E. Knox, J.B. Cross, V. Bakken, C. Adamo, J. Jaramillo, R. Gomperts, R.E. Stratmann, O. Yazyev, A.J. Austin, R. Cammi, C. Pomelli, J.W. Ochterski, R.L. Martin, K. Morokuma, V.G. Zakrzewski, G.A. Voth, P. Salvador, J.J. Dannenberg, S. Dapprich, A.D. Daniels, O. Farkas, J.B. Foresman, J.V. Ortiz, J. Cioslowski, D.J. Fox, Gaussian 09, Revision D.01, Gaussian Inc., Wallingford, CT, 2009.
[31] M. Cossi, N. Rega, G. Scalmani, V. Barone, J. Comput. Chem. 24 (2003) 669.
[32] J. Tomasi, B. Mennucci, R. Cammi, Chem. Rev. 105 (2005) 2999.
[33] G. Scalmani, M.J. Frisch, J. Chem. Phys. 132 (2010) 114110.
[34] P. Šimůnek, M. Svobodová, V. Bertolasi, V. Macháček, Synthesis 11 (2008) 1761.
[35] A.O. Terentev, V.A. Vil, I.A. Yaremenko, O.V. Bityukov, D.O. Levitsky, V.V. Chernyshev, G.I. Nikishin, F. Fleur, New J. Chem. 38 (2014) 1493.
[36] O.S. Shneider, E. Pisarevsky, P. Fristrup, A.M. Szpilman, Org. Lett. 17 (2015) 282.
[37] I. Adachi, K. Harada, R. Miyazaki, H. Kano, Chem. Pharm. Bull. 22 (1974) 61.
[38] N.M.D. Brown, P. Bladon, J. Chem. Soc. A (1969) 526.